Optical Activity of Hemoproteins in the Soret Region. Circular Dichroism of the Heme Undecapeptide of Cytochrome *c* in Aqueous Solution†

Gideon Blauer,‡ Narasimha Sreerama, and Robert W. Woody*

Department of Biochemistry, Colorado State University, Fort Collins, Colorado 80523

Received October 7, 1992; Revised Manuscript Received April 13, 1993

ABSTRACT: Different possible mechanism for generation of optical activity of hemoproteins in the Soret region are reconsidered. The heme undecapeptide of cytochrome *c* does not contain aromatic amino acid residues, so its considerable optical activity cannot be due to coupling of heme $\pi\pi^*$ transitions with those of aromatic residues. CD data for the heme undecapeptide and for ferrimyoglobin and some of their complexes with small molecules are presented and critically compared. Symmetrically coordinated imidazole complexes show rotational strengths of the same magnitude as those of corresponding nonsymmetrically coordinated compounds. Inherent chirality in the bound heme is inferred to be a significant source of optical activity in the heme undecapeptide. Theoretical calculations based upon a molecular dynamics simulation support this proposal. Coupled oscillator interactions with the peptide $\pi\pi^*$ transitions and with the high-energy transitions in the peptide groups and thioether sulfurs, as modeled by polarizabilities, also make significant contributions. These same mechanisms must also be considered in hemoproteins in general.

The optical activity of hemoproteins near 400 nm (Soret region), as initially measured by ORD[1] and subsequently by CD, generally gives rise to a Cotton effect of appreciable magnitude. Molar ellipticities of the order of 10^5 deg cm^2 dmol^{-1}, based on heme, have been measured for ferrimyoglobin [see, for example, Sugita *et al.* (1971)] and hemoglobin derivatives [see, for example, Ruckpaul *et al.* (1970)]. The corresponding rotational strengths have been reported to be about 0.5 and 0.2 DBM per heme, respectively. The optical activity of these and other hemoproteins such as cytochrome *c*, cytochrome oxidase, and horseradish peroxidases has been reviewed (Myer & Pande, 1978; Blauer, 1974). The presently accepted mechanism for the generation of optical activity in the Soret region is based on the coupling of the heme $\pi\pi^*$ electric dipole transition moments with those of proximate aromatic amino acid residues of the protein, leading to a net rotational strength comparable to the experimentally observed values (Hsu & Woody, 1971).

The heme undecapeptide of horse heart cytochrome *c* (microperoxidase) does not contain aromatic amino acid residues other than a single histidyl residue. However, in the nonaggregated state, it exhibits an optical activity in the Soret region (Urry, 1967) which is of the same order of magnitude as that measured for myoglobin and other hemoproteins. It therefore seemed of interest to reinvestigate the optical activity of the heme undecapeptide and some of its complexes to gain more insight into possible mechanisms of generation of optical activity in this peptide and in hemoproteins in general.

MATERIALS AND METHODS

Materials. Heme undecapeptide (microperoxidase) disodium salt from equine heart cytochrome *c* was obtained from Sigma (lot 10H7230). Myoglobin (horse heart), lyophilized, was also a Sigma product (lot 69F7170). Addition of a slight molar excess of potassium ferricyanide to either microperoxidase or myoglobin solutions did not significantly affect the respective Soret absorptions, indicating that the predominant form was ferric in both cases. Imidazole was purchased from Sigma (lot 128F-5084). All reagents used in this work were of analytical grade.

Concentration Determination. Concentrations of heme undecapeptide solutions were determined spectrophotometrically by conversion of the heme peptide to its ferrohemochrome in 25% (v/v) pyridine–0.1 M aqueous sodium hydroxide by addition of solid sodium dithionite (Paul *et al.*, 1953). An ϵ value of 29.1 mM^{-1} cm^{-1} for the α-band maximum observed at 550 nm was used (Morton, 1958). In some cases, an ϵ value of 116 mM^{-1} cm^{-1} for the Soret band maximum of 407 nm, as determined independently by the hemochrome method, was used for calculations of the heme peptide concentration.

Instrumentation. CD measurements were carried out on a Jasco J-41C instrument at 24 ± 1 °C using (+)-10-camphorsulfonic acid for daily calibration, assuming $[\theta]_{290.5}$ = 7800 deg cm^2 dmol^{-1} (Chen & Yang, 1977). For light absorption measurments, a Cary 118 spectrophotometer was used. Water was the reference solvent in all measurements. Rectangular cells with 1.0 and 0.1 cm path lengths were used, depending on the heme concentration. In most CD experiments reported, the absorbance of the solution was less than 1, and in no case did it exceed 1.3.

The molar ellipticity [Θ] is given in deg cm^2 dmol^{-1}, calculated per heme. In the case of associated hemes, [Θ] may depend on the heme concentration, which is specified in each case. Rotational strengths were estimated by tracing the CD curves onto graph paper, followed by cutting and weighing the areas to be integrated. The wavelength interval was from 460 to 360 nm or the crossover point, if that occurred above 360 nm. Thus, the reported rotational strengths may include contributions from transitions other than the Soret transitions, but the extraneous contributions are expected to be small.

Molecular Dynamics Simulations and CD Calculations. MD simulations in vacuum were performed using the GROMOS program package and united atom parameters (van

† Supported by NIH Grant GM22994 to R.W.W.

‡ On leave of absence from the Hebrew University, Jerusalem.

[1] Abbreviations: CD, circular dichroism; CTAB, cetyltrimethylammonium bromide; DBM, Debye–Bohr magneton (1 DBM = 0.9273 × 10^{-38} erg cm^3); HUP, heme undecapeptide from cytochrome *c*; MD, molecular dynamics; ORD, optical rotatory dispersion.

0006-2960/93/0432-6674$04.00/0

Gunsteren & Berendsen, 1988). All calculations were performed on a Silicon Graphics Iris 4D workstation. The standard GROMOS parametrization does not include any constraints on improper dihedrals for torsion about the partial double bonds within the pyrrole rings of the porphyrin, although contraints are provided to maintain planarity at each atom. The necessary improper dihedrals have been incorporated in the present calculations, using a force constant of 40 kcal mol^{-1} rad^{-2} for the harmonic potential, the same value used in other aromatic systems. Bond lengths were constrained using the SHAKE algorithm (van Gunsteren & Berendsen, 1977), and a time step of 2 fs was used. The nonbonded pair list was generated using a residue-based cutoff of 8.0 Å and updated every 20 steps. The temperature was maintained at 300 K during the simulation by coupling to a heat bath (Berendsen *et al.*, 1984) with relaxation time $\tau = 0.1$ ps. The initial structure was taken from the crystal structure (Takano & Dickerson, 1980) of the corresponding fragment of tuna ferricytochrome *c* [data file pdb3cyt.ent of the Protein Data Bank (Abola *et al.*, 1987)] and subjected to energy minimization by the method of steepest descents. (The sequence of tuna heme undecapeptide is identical to that of horse.) The resulting structure was equilibrated for 20 ps, and MD data were collected for 1000 ps.

The rotational strength of the Soret band was calculated from the MD structures at 1-ps intervals. The intrinsic heme contribution was calculated in the Pariser–Parr–Pople approximation (Murrell, 1963) using a modified version (Smith & Woody, 1976) of the program SCFCIO (Bloor & Gilson, 1965). The heme π-electron system was treated as a porphyrin dianion, using the "standard" parameters of Weiss *et al.* (1965). Configuration interaction included 32 configurations with differences in orbital energies of less than *ca.* 9 eV. Examination of the CI coefficients showed that the visible and Soret bands conform closely to Gouterman's four-orbital model (Weiss *et al.*, 1965). For each structure in the trajectory, the transition energies, transition dipole moments, and rotational strengths of the heme Soret bands were calculated. Transition monopoles (Tinoco, 1962) were generated for use in calculating coupling with transitions in other groups.

In addition to the intrinsic heme contributions, coupling of the heme Soret electric dipole transition moments with the peptide $\pi\pi^*$ and $n\pi^*$ transitions and the $\pi\pi^*$ transitions of the histidyl imidazole were considered, following the methods of Hsu and Woody (1971). Transition monopoles for the heme transitions were generated for each heme structure on the trajectory. The transition monopole charges for the peptide and imidazole groups were kept constant throughout the calculations, but their positions followed the MO trajectory.

An additional contribution not explored in detail by Hsu and Woody (1971) was also considered in this calculation—that of high-energy transitions in the peptide groups and in the thioether sulfurs. These contributions were calculated using the following expression:

$$(R_A)_j = \frac{\pi}{\lambda_a}\frac{\nu_0^2}{\nu_0^2-\nu_a^2}\left\{(\alpha_{33}-\alpha_{11})_j\sum_t \frac{q_{it0a}(\mathbf{R}_{it0a;j}\cdot\mathbf{e}_{3j})(\mathbf{e}_{3j}\cdot\mu_{i0a}\times\mathbf{R}_{ij})}{R^3_{it0a;j}} + (\alpha_{ii})_j\sum_t \frac{q_{it0a}\mathbf{R}_{it0a;j}\cdot\mu_{i0a}\times\mathbf{R}_{ij}}{R^3_{itoa;j}}\right\}$$

Here, λ_a is the wavelength of the transition $0 \rightarrow a$, ν_a is its frequency, and ν_0 is an average frequency for the high-energy transitions contributing to the polarizability, which we have taken to be 10^5 cm^{-1}. The quantity q_{it0a} is a transition monopole charge, centered at atom *t*, for a heme $\pi\pi^*$ transition, associated with the electric dipole transition moment μ_{i0a}. $\mathbf{R}_{it0a;j}$ is the vector from the monopole to the center of the polarizable group *j*, and $R_{it0a;j}$ is the scalar distance. $\mathbf{R}_{ij}$ is the vector from the center of the heme to the center of the polarizable group. Group *j* is treated as an axially symmetric polarizable group with polarizabilities $(\alpha_{33})_j$ and $(\alpha_{11})_j$ parallel and perpendicular, respectively, to the symmetry axis, which is in the direction of the unit vector $\mathbf{e}_{3j}$. Thus, $(\alpha_{33} - \alpha_{11})_j$ is the anisotropy of the polarizability. This equation was derived by the methods described by Woody and Tinoco (1967).

The thioether sulfurs were treated as isotropic polarizable groups with $\alpha_{11} = 3.06$ Å^3, calculated from the atomic refraction (Weast, 1972). The peptide group polarizability is not well characterized. Three different sets of parameters were used. Model I is that of Woody and Tinoco (1967), in which $(\alpha_{33} - \alpha_{11}) = -0.61$ Å^3, $\alpha_{11} = 3.03$ Å^3, and $\mathbf{e}_3$ is normal to the amide plane. Model II also has $\mathbf{e}_3$ normal to the amide plane but has $(\alpha_{33} - \alpha_{11}) = -4.63$ Å^3 and $\alpha_{11} = 5.63$ Å^3. This model was derived from the data of Khanarian *et al.* (1981) for *N*-methylacetamide, corrected for the contributions of the two methyl groups, assumed to be isotropic (LeFevre & LeFevre, 1955). Model III was derived from the polarizability ellipsoid calculated for the O=CNH group using the atom dipole interaction method and parameters of Applequist *et al.* (1972). The contributions of the peptide $\pi\pi^*$ transition were then subtracted from the appropriate elements of the polarizability matrix, and the matrix was diagonalized. The three components in the principal axis system were 5.28, 1.34, and 1.20 Å^3. The two smaller components were averaged to give an axially symmetric tensor with $(\alpha_{33} - \alpha_{11}) = 4.01$ Å^3 and $\alpha_{11} = 1.27$ Å^3. The symmetry axis $\mathbf{e}_3$ is rotated 14° from the carbonyl bond direction toward the C^α–C' bond direction.

RESULTS

Under the present conditions of measurement (peptide concentration $\approx 1 \times 10^{-4}$ M; 0.05 M sodium borate buffer, pH 9.1, room temperature), positive CD bands were observed for the ferriheme undecapeptide at 417 and 398 nm and a negative band was observed at 408 nm, in agreement with previous data obtained under different conditions (Urry, 1967). Also, the ferroheme undecapeptide showed CD extrema at 425, 420 (negative), and 415 nm, respectively. Upon dilution at pH 9.1 of the ferriheme peptide (2.2×10^{-4} M) by a factor of 75, a single CD band centered at 398 nm was obtained [see also Urry (1967)]. Surprisingly, the carbon monoxide complex of ferroheme undecapeptide in aqueous buffer showed two proximate bands of opposite sign in the Soret region [Figure 1; observed extrema at 416 nm (negative) and 406 nm (positive)]. Upon 40-fold dilution, a single positive CD band centered at 409 nm was observed (Figure 1), indicating exciton interactions of an aggregated system at the higher peptide concentration. On the other hand, only a single CD band was observed at 414 nm for the CO complex in the presence of 2% (w/v) of CTAB in the higher concentration range of the ferroheme undecapeptide (1.1×10^{-4} M), while the ferriheme undecapeptide showed two proximate bands of opposite sign under similar conditions[2] [extrema at 412 nm (positive) and 398 nm (negative), respectively].

In Figure 2, CD spectra of both ferri- and ferroheme undecapeptide in the presence of 0.1 M imidazole are presented. In each case, only one dominant band is observed in the Soret region [see Urry (1967)], although small additional bands appear to be present under the conditions given. The

[2] In agreement with unpublished results by T. G. Traylor and G. Blauer.

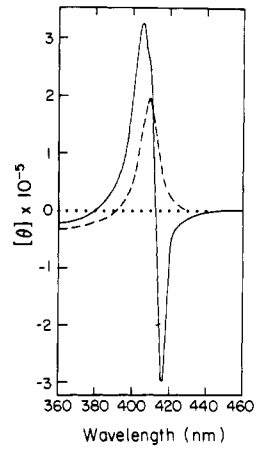

FIGURE 1: CD spectrum of the CO complex of reduced heme undecapeptide at two different concentrations: (—) 6.2×10^{-5} M; (- - -) 1.5×10^{-6} M. Reduction of the aqueous peptide solution in 0.05 M sodium borate buffer was effected by solid sodium dithionite. Carbon monoxide was then bubbled through the solution. The more concentrated sample was diluted into a buffer solution treated previously with sodium dithionite and CO. Both samples had a final pH of 7.4.

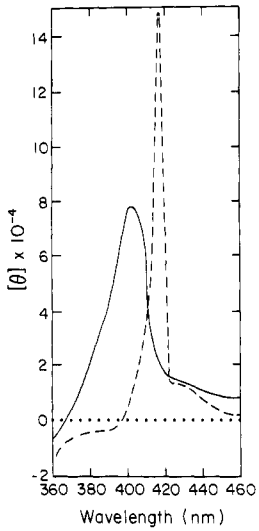

FIGURE 2: CD spectrum of the heme undecapeptide from equine heart cytochrome *c* in the presence of 0.1 M imidazole in aqueous solution: (—) ferric; (- - -) reduced with solid sodium dithionite, pH 9 (0.05 M sodium borate buffer) (pH 8.4 after reduction). Undecapeptide concentration was 7.3×10^{-5} M.

light absorption spectra in the visible region of the ferroheme peptide showed typical ferroheme maxima at 550 and 520 nm, respectively.

For the purpose of considerations with regard to ligand symmetry to be presented below, ferrimyoglobin–imidazole complexes were also studied. In Figure 3, a comparison of CD spectra in both the presence and absence of imidazole is presented. In the former case, the Soret band is shifted from 409 to 417 nm under the conditions given. Between 500 and 600 nm, a distinct and typical light absorption maximum at 534 nm and a shoulder near 560–570 nm are recorded for the ferrihemochrome, as for the analogous ferrihemoglobin–imidazole complex (Antonini & Brunori, 1971), while the Soret maximum is located at 414 nm.

In Table I, results are summarized for those cases in which a single major CD band was observed in the Soret region. The rotational strength of the ferriheme undecapeptide is comparable in magnitude to that of ferrimyoglobin. There is no large difference in the rotational strength of ferrimyoglobin or the ferriheme peptide in either the absence or presence of

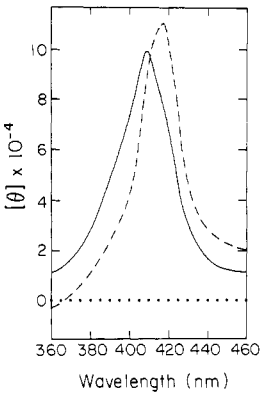

FIGURE 3: CD spectrum of horse heart myoglobin (6.4×10^{-5} M; see Table I) in the Soret region, both in the absence (—) and in the presence (- - -) of 0.1 M imidazole in aqueous solution, pH 9 (0.05 M sodium borate buffer). Similar results were obtained in the presence of 0.26 M imidazole.

0.1 M imidazole in each case. However, in the presence of imidazole, the rotational strength is considerably smaller for the ferroheme undecapeptide as compared to the ferric peptide, although the molar ellipticity of the Soret band is about twice as large in the reduced form, which exhibits a narrow band (Figure 2).

The rotational strength reported here for equine ferrimyoglobin (0.73 DBM) is significantly larger than the previously reported values of 0.45 DBM for sperm whale ferrimyoglobin (Willick *et al.*, 1969) and 0.48 DBM for the bovine protein (Moench, 1986) or the values estimated from published reports for sperm whale ferrimyoglobin, 0.54 DBM (Beychok, 1967), and for equine ferrimyoglobin, 0.42 DBM (Sugita *et al.*, 1971). However, only the data of Sugita *et al.* refer to the equine protein. Moreover, variations in pH, wavelength region included in the Soret region, and CD instrument calibration as well as uncertainties in the protein concentration determination can lead to significant variability. For the present study, the comparison between the protein in the presence and absence of imidazole is the point of interest.

Figure 4 shows the structures of the heme from the crystal structure of tuna ferricytochrome *c* (Takano & Dickerson, 1980) and as obtained from MD at intervals of 200 ps. The structures are shown in the plane containing one of the pyrrole rings not containing the thioether groups. The deviations from planarity of the heme can be clearly seen. The heme in cytochrome *c* is significantly distorted, and the structures from the MD simulation have qualitatively similar distortions, although the amplitude of the distortions is greater in the simulated structures. The calculated intrinsic heme and total rotational strengths for these structures are also shown in Figure 4. These are all positive and of the order of magnitude of that observed for the heme peptide (+0.55 DBM).

The contributions to the Soret rotational strength of other mechanisms are shown in Table II. The histidyl imidazole $\pi\pi^*$ and the peptide $n\pi^*$ transitions make negligible contributions to the net Soret rotational strength, although the former contribute significantly to the individual Soret components. The peptide $\pi\pi^*$ transitions give rise to a substantial negative rotational strength in the Soret band. The polarizability contributions are also significant. That of the thioether sulfurs is positive, while those of the peptide groups depend strongly on the model chosen. Models I and II with symmetry axis normal to the amide plane have little net impact on the calculated Soret rotational strength, but this is due to extensive cancellation of opposing effects on the individual components. Model III, in which the symmetry axis is roughly along the C=O bond direction, makes a sizeable positive contribution

Table I: CD Data for Soret Region[a]

system	λ_{max} (nm)	$[\theta]_{max} \times 10^{-4}$ deg cm^2 dmol^{-1}	approx rotational strength (DBM)
ferri-HUP,[b] 2.9×10^{-6} M[c]	398	9.8	0.55
ferro-HUP, 1.5×10^{-6} M[d] + CO	409	20	0.48
ferro-HUP, 1.1×10^{-4} M + CTAB + CO	414	16	0.38
ferri-HUP, 7.3×10^{-5} M + 0.1 M imidazole	402	7.8	0.44
ferro-HUP, 7.3×10^{-5} M + 0.1 M imidazole[e]	417	15	0.26
ferrimyoglobin, 6.4×10^{-5} M[f]	409	10	0.73
ferrimyoglobin, 6.4×10^{-5} M + 0.1 M imidazole	417	11	0.69

[a] 360–460 nm. All systems were measured in aqueous 0.05 M borate buffer, pH 9, except when stated otherwise. [b] HUP, heme undecapeptide. [c] Diluted from higher concentration. [d] pH 7.5. [e] pH 8.4. [f] Calculated on the basis of $\epsilon_{409} = 1.35 \times 10^5$ M^{-1} cm^{-1}.

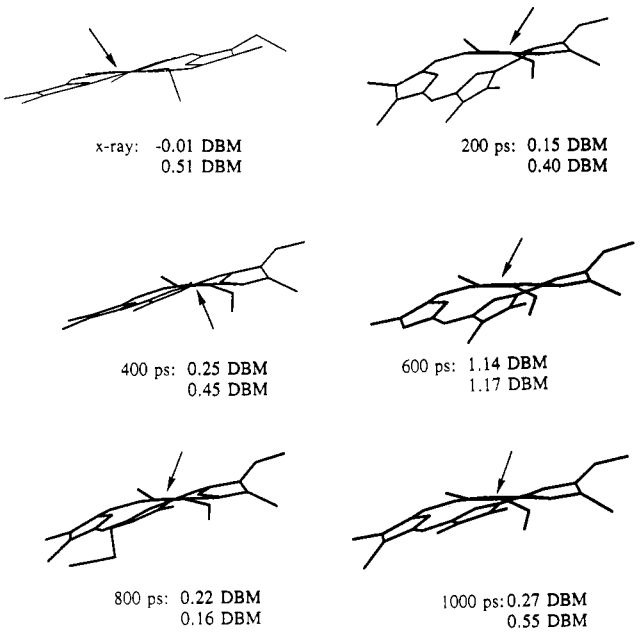

FIGURE 4: Snapshots of the heme in heme undecapeptide taken from the crystal structure of tuna ferricytochrome *c* (Takano & Dickerson, 1980) and at intervals of 200 ps during an MD simulation. The plane of one of the pyrrole rings not containing the thioether groups is toward the viewer and is shown as the horizontal line indicated by the arrow. For each structure, the calculated intrinsic heme (upper) and total (lower) rotational strengths are given.

Table II: Contributions to the Rotational Strength of the Soret Band in Heme Undecapeptide[a]

contributions to the rotational strength	Soret component 1[b]	Soret component 2	Soret band
intrinsic heme	−0.3803	0.5575	0.1772
histidine $\pi\pi^*$	0.1109	−0.1317	−0.0208
peptide $n\pi^*$	−0.0059	−0.0068	−0.0126
peptide $\pi\pi^*$	−0.2341	−0.0860	−0.3201
sulfur polarizability	0.3027	−0.1463	0.1564
amide polarizability[c]			
model I	0.0857	−0.0700	0.0157
model II	−0.1494	0.1098	−0.0396
model III	0.2727	−0.0713	0.2014
total			
model I	−0.1209	0.1167	−0.0042
model II	−0.3560	0.2965	−0.0595
model III	0.0661	0.1154	0.1815

[a] Theoretical rotational strength contributions are reported as the average over a 1000-ps MD simulation (in Debye–Bohr magnetons). [b] Component 1 is the lower energy component of the Soret band, and component 2 is the higher energy component. These were averaged separately over the MD trajectory. [c] See text for the description of models I–III.

to the Soret rotational strength. Of the three models, only model III gives a net rotational strength (+0.18) which is in qualitative agreement with experiment (+0.55). It should also be noted that model III gives rotational strengths for

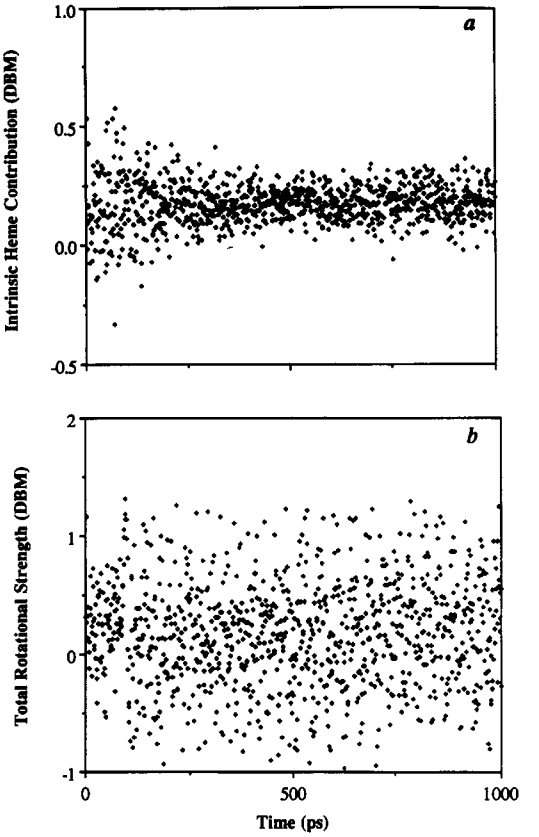

FIGURE 5: Plot of calculated rotational strengths of the Soret band of the heme of HUP during the MD simulation: (a) intrinsic heme contribution; (b) total rotational strength.

both Soret components which are positive, so a single positive CD band is predicted. The other two models predict that the two components will have opposite signs and comparable magnitudes. As discussed by Hsu and Woody (1971), this would lead to a couplet in the CD spectrum, contrary to observation.

Figure 5 shows a plot of the intrinsic heme rotational strength of the Soret band during the 1000-ps simulations and the total calculated rotational strength using model III for the peptide polarization. It is evident from Figure 5a that there is a bias in the intrinsic heme contribution toward positive rotational strength. The positive bias for the total rotational strength is more subtle, though real. The fluctuations are large (± *ca.* 1 DBM) throughout the 1000 ps of the simulation. The average rotational strength over 1000 structures is 0.18 DBM. This, though of correct sign, is lower than the experimentally observed value (0.55 DBM; Table I).

DISCUSSION

The change of multiple CD bands of opposite sign to an apparently single band upon dilution or ligand addition has been attributed to disaggregation of the heme peptide (Urry,

1967; Ehrenberg & Theorell, 1955). This is also apparent from the present data on the CO complex of the heme undecapeptide in aqueous solution in the absence of detergent (Figure 1). If indeed the two proximate CD bands of opposite sign observed for this complex at the higher peptide concentrations are due to exciton interactions between heme molecules within an aggregate, it is not obvious why, at similar ferroheme peptide concentrations, imidazole as an additional ligand causes disaggregation (absence of exciton interactions, see Figure 2). It appears that the CO complex is more easily accommodated within a peptide dimer or higher aggregate.

For the aggregated heme undecapeptide, exciton interactions between heme moieties within chiral aggregates determined by the chiral amino acids have been postulated as a source for generation of the observed Cotton effects (Urry, 1967). However, the origin of the optical activity of the monomeric heme undecapeptide and its complexes requires further consideration. The heme undecapeptide of horse heart cytochrome *c* has no aromatic amino acid residues and contains only a single histidyl. Therefore, the mechanism for the generation of optical activity in the Soret region which is generally applied to hemoproteins and is based on the coupling of $\pi\pi^*$ electric dipole transition moments with those of aromatic amino acid residues (Hsu & Woody, 1971) cannot operate in the case of the heme undecapeptide. Coupled oscillator interactions of the heme with the single proximal histidyl residue (imidazole) were predicted (Hsu & Woody, 1971) to lead to rotational strengths of nearly equal magnitude and opposite sign for the two Soret components and thus yield only a small net rotational strength. This should generally be the case for proximal histidines with their plane nearly orthogonal to that of the heme and is verified for the heme undecapeptide by the calculations described here (Table II).

It has been suggested (Myer & Pande, 1978) that the low symmetry resulting from the binding of different axial ligands to the heme *c* of the undecapeptide constitutes a major source for generation of the Soret optical activity. The present data (Table I) show that with identical axial ligands (imidazole) in both ferriheme u: decapeptide and ferrimyoglobin, rotational strengths are obtained in the Soret region which are similar to those for the corresponding nonsymmetrical complexes. Therefore, symmetry considerations at the coordinating heme iron could not account for the magnitude of the Cotton effects observed.

Alternatively, the optical activity observed in the heme undecapeptide of cytochrome *c* may arise from one or more mechanisms not considered by Hsu and Woody (1971) or predicted to be negligible for myoglobin and hemoglobin. Inherent chirality in the heme is one of the neglected mechanisms. Hsu and Woody (1971) recognized that chiral distortions of the heme are a possible source of optical activity, but the only information available at that time concerned torsion of the vinyl groups, which they predicted to make only minor contributions. More refined calculations (Woody, 1978) on the effects of out-of-plane twisting of the vinyl groups and doming of the plane indicated potentially significant contributions, but the results depended strongly on the nature of the deformations, which were still poorly defined by X-ray diffraction data.

Moench (1986) pointed out that if certain types of deformation make dominant contributions to the CD of a heme protein, the CD spectrum should be approximately a mirror image when the heme is rotated by 180° about an in-plane axis, as in the case of heme isomerism (La Mar *et al.*, 1978). Although not mirror images, the Soret CD spectra of the two heme isomers in sperm whale (carbonmonoxy)-myoglobin (MbCO) are apparently opposite in sign (Aojula *et al.*, 1988), suggesting a substantial contribution from inherent chirality of the heme. This has been supported by recent theoretical calculations on the two isomers of MbCO (Woody and van Gunsteren, unpublished results).

Free unbound heme is not optically active because of the plane of symmetry in its ensemble-average structure. However, when bound to a chiral macromolecule, small but systematic distortions from planarity could generate significant rotational strength in the heme transitions. It is well established from studies of model porphyrins (Hoard, 1971; Scheidt & Lee, 1987) that hemes can exhibit significant deviations from planarity. Refinements of high-resolution X-ray structures for heme proteins have revealed distortions from planarity of the heme in several cytochromes *c* (Takano & Dickerson, 1981a,b; Matsuura *et al.*, 1982; Higuchi *et al.*, 1984; Louie & Brayer, 1990; Bushnell *et al.*, 1990). In the refinements, each pyrrole ring is constrained to be planar, but the orientation of the pyrrole planes is not constrained. These high-resolution structures show that the hemes in all cytochrome *c* molecules studied thus far have a saddle shape with deviations as large as 15° between the normals to the pyrroles and the normal to the mean plane of the heme. Interestingly, the deviations are largest for the pyrroles through which the thioether linkages are made.

The heme undecapeptide retains the thioether linkages and the histidyl coordinated to the heme iron. These three points of attachment may suffice to induce a systematic deviation from planarity in the heme in solutions of the heme undecapeptide. The results of the molecular dynamics simulation (Figures 4 and 5) show that a time-average chirality is retained in aqueous solution, giving a predicted intrinsic heme rotational strength which is of the same sign and order of magnitude as that observed for the heme undecapeptide.

Heme nonplanarity can also contribute to the optical activity of proteins containing protoheme, in which the heme–protein interactions are strictly noncovalent. Deviations from planarity in the porphyrin core have been seen in the high-resolution structures of a number of protoheme-containing proteins, e.g., erythrocruorin (Steigemann & Weber, 1979), sperm whale oxymyoglobin (Phillips, 1980), and horse heart metmyoglobin (Evans & Brayer, 1990). Recently, the ellipticity of horse heart apomyoglobin reconstituted with the symmetrical protoheme XIII was found to be significantly weaker than that of the native protein, especially in the ferric state (Santucci *et al.*, 1990). These lower ellipticities were attributed to the high symmetry of heme XIII but could also be due to the bound heme adopting a more nearly planar conformation.

Recent work on metal complexes of an etioporphyrin I derivative which is distorted from planarity by steric repulsion among its substituents and can be resolved into its optical antipodes (Konishi *et al.*, 1990) is considered to be relevant to the general topic of nonplanar porphyrins.

A second mechanism which Hsu and Woody (1971) did not consider explicitly is that of coupling of the heme $\pi\pi^*$ transitions with higher energy transitions, which can be approximated by interaction with polarizable groups (Tinoco, 1962). Hsu and Woody did consider high-energy transitions in alkyl groups near the heme, but approximated these as $\sigma\sigma^*$ transitions following the model of Raymonda and Simpson (1967). They found the contribution of coupling with these $\sigma\sigma^*$ transitions to be negligible for myoglobin and hemoglobin. However, the contributions of amide groups may be much larger because of their anisotropy, whereas alkyl groups are only weakly anisotropic (LeFevre & LeFevre, 1955). Fur-

thermore, two thioether sulfurs are present in the heme undecapeptide, and they may be important because of their high polarizability and proximity to the heme. Our calculations indicate that these sources of rotational strength are important, especially if the peptide polarizability is described by model III, with the C=O bond direction as the most polarizable direction, with smaller polarizabilities in the out-of-plane direction and the in-plane direction normal to the C=O bond. Because this is the only model which leads to qualitative agreeement with experiment, we prefer this model.

The peptide $\pi\pi^*$ transition was considered by Hsu and Woody (1971) but made only a small net contribution for sperm whale myoglobin and horse hemoglobin. However, subsequent calculations on erythrocruorin (Strassburger *et al.*, 1978) and on more highly refined myoglobin structures (Woody, unpublished results) have indicated that the peptide $\pi\pi^*$ contribution may be significant, although smaller than the heme–aromatic coupling effect in these proteins. In the case of heme undecapeptide, coupling with the peptide $\pi\pi^*$ transition may be relatively more important because the heme is not surrounded by peptide groups, which would tend to average out the effects in a heme protein. Our calculations bear out this conjecture, because the largest single contribution to the heme undecapapetide CD is that of the peptide $\pi\pi^*$ transitions, albeit of the opposite sign to that of the observed CD band.

Thus, as in the case of myoglobin, hemoglobin, and other heme proteins (Hsu & Woody, 1971; Strassburger *et al.*, 1978), the rotational strength observed in the heme undecapeptide is the result of a number of contributions. Whereas in the heme proteins coupling of the heme $\pi\pi^*$ transitions with aromatic side-chain transitions appears to be dominant, several different mechanisms, all of comparable magnitude, are effective in making the heme of the heme undecapeptide optically active. However, as shown by our experimental data, asymmetry in the ligand field strength does not play a significant role. The present results also suggest that inherent chirality in the heme and polarizable groups contributions must be considered as potentially significant determinants of the optical activity of heme proteins.

REFERENCES

Abola, E. E., Bernstein, F. C., Bryant, H. H., Koetzle, T. F., & Weng, J. (1987) in *Crystallographic Databases—Information Content, Software Systems, Scientific Applications* (Allen, F. G., & Sievers, R., Eds.) pp 107–132, Data Commission of the International Union of Crystallography, Cambridge, U.K.

Antonini, E., & Brunori, M. (1971) *Hemoglobin and Myoglobin in their Reactions with Ligands*, p 45, North-Holland, Amsterdam.

Aojula, H. S., Wilson, M. T., Moore, G. R., & Williamson, D. J. (1988) *Biochem. J. 250*, 853–858.

Applequist, J., Carl, J. R., & Fung, K.-K. (1972) *J. Am. Chem. Soc. 94*, 2952–2960.

Berendsen, H. J. C., Postma, J. P. M., van Gunsteren, W. F., DiNola, A., & Haak, J. R. (1984) *J. Chem. Phys. 81*, 3684–3690.

Beychok, S. (1967) in *Poly-α-Amino Acids* (Fasman, G. D., Ed.) pp 293–337, Marcel Dekker, New York.

Blauer, G. (1974) *Struct. Bonding (Berlin) 18*, 69–129.

Bloor, J. E., & Gilson, B. R. (1965) *QCPE 71.2*.

Bushnell, G. W., Louie, G. V., & Brayer, G. D. (1990) *J. Mol. Biol. 214*, 585–595.

Chen, G. C., & Yang, J. T. (1977) *Anal. Lett. 10*, 1195–1207.

Ehrenberg, A., & Theorell, H. (1955) *Acta Chem. Scand. 9*, 1193–1205.

Evans, S. V., & Brayer, G. D. (1990) *J. Mol. Biol. 213*, 885–897.

Higuchi, Y., Kusunoki, M., Matsuura, Y., Yasuoka, N., & Kakudo, M. (1984) *J. Mol. Biol. 172*, 109–139.

Hoard, J. L. (1971) *Science 174*, 1295–1302.

Hsu, M. C., & Woody, R. W. (1971) *J. Am. Chem. Soc. 93*, 3515–3525.

Khanarian, G., Mack, P., & Moore, W. J. (1981) *Biopolymers 20*, 1191–1209.

Konishi, K., Miyazaki, K., Aida, T., & Inoue, S. (1990) *J. Am. Chem. Soc. 112*, 5639–5640.

La Mar, G. N., Budd, D. L., Viscio, D. B., Smith, K. M., & Langry, K. C. (1978) *Proc. Natl. Acad. Sci. U.S.A. 75*, 5755–5759.

LeFevre, C. G., & LeFevre, R. J. W. (1955) *Rev. Pure Appl. Chem. 5*, 261–318.

Louie, G. V., & Brayer, G. D. (1990) *J. Mol. Biol. 214*, 527–555.

Matsuura, Y., Takano, T., & Dickerson, R. E. (1982) *J. Mol. Biol. 156*, 389–409.

Moench, S. J. (1986) Ph.D. thesis, Colorado State University, Fort Collins, CO.

Morton, R. K. (1958) *Rev. Pure Appl. Chem. 8*, 161–220.

Murrell, J. N. (1963) *The Theory of the Electronic Spectra of Organic Molecules*, pp 108–115, Methuen, London.

Myer, Y. P., & Pande, A. (1978) in *The Porphyrins* (Dolphin, D., Ed.) Vol. III, pp 271–322, Academic Press, New York.

Paul, K. G., Theorell, H., & Akeson, A. (1953) *Acta Chem. Scand. 7*, 1284–1287.

Phillips, S. E. V. (1980) *J. Mol. Biol. 142*, 531–554.

Raymonda, J. W., & Simpson, W. T. (1967) *J. Chem. Phys. 47*, 430–448.

Ruckpaul, K., Rein, H., Ristau, O., & Jung, F. (1970) *Biochim. Biophys. Acta 221*, 9–19.

Santucci, R., Ascoli, F., La Mar, G. N., Parish, D. W., & Smith, K. M. (1990) *Biophys. Chem. 37*, 251–255.

Scheidt, W. R., & Lee, Y. J. (1987) *Struct. Bonding (Berlin) 64*, 1–70.

Smith, J. C., & Woody, R. W. (1976) *J. Phys. Chem. 80*, 1094–1100.

Steigemann, E., & Weber, E. (1979) *J. Mol. Biol. 127*, 309–338.

Strassburger, W., Wollmer, A., Thiele, H., Fleischhauer, J., Steigemann, W., & Wilson, E. (1978) *Z. Naturforsch. 33C*, 908–911.

Sugita, Y., Nagai, M., & Yoneyama, Y. (1971) *J. Biol. Chem. 246*, 383–388.

Takano, T., & Dickerson, R. E. (1980) *Proc. Natl. Acad. Sci. U.S.A. 77*, 6371–6375.

Takano, T., & Dickerson, R. E. (1981a) *J. Mol. Biol. 153*, 79–94.

Takano, T., & Dickerson, R. E. (1981b) *J. Mol. Biol. 153*, 95–115.

Tinoco, I., Jr. (1962) *Adv. Chem. Phys. 4*, 113–160.

Urry, D. W. (1967) *J. Am. Chem. Soc. 89*, 4190–4196.

van Gunsteren, W. F., & Berendsen, H. J. C. (1977) *Mol. Phys. 34*, 1311–1327.

van Gunsteren, W. F., & Berendsen, H. J. C. (1988) GROMOS, Biomos BV, University of Groningen, Groningen, Netherlands.

Weast, R. C., Ed. (1972) *CRC Handbook of Chemistry and Physics*, 53rd ed., p E-209, Chemical Rubber Co., Cleveland, OH.

Weiss, C., Kobayashi, H., & Gouterman, M. (1965) *J. Mol. Spectrosc. 16*, 415–450.

Willick, G. E., Schonbaum, G. R., & Kay, C. M. (1969) *Biochemistry 8*, 3729–3734.

Woody, R. W. (1978) in *Biochemical and Clinical Aspects of Hemoglobin Abnormalities* (Caughey, W. S., Ed.) pp 279–298, Academic Press, New York.

Woody, R. W., & Tinoco, I., Jr. (1967) *J. Chem. Phys. 46*, 4927–4945.